Journal of Magnetism and Magnetic Materials 417 (2016) 407–412

Contents lists available at ScienceDirect

Journal of Magnetism and Magnetic Materials

journal homepage: www.elsevier.com/locate/jmmm

Magneto-structural studies of sol–gel synthesized nanocrystalline manganese substituted nickel ferrites

R.S. Pandav [a], R.P. Patil [b], S.S. Chavan [a], I.S. Mulla [c], P.P. Hankare [a,*]

[a] Department of Chemistry, Shivaji University, Kolhapur 416004, MH, India
[b] Department of Chemistry, M.H. Shinde Mahavidyalaya, Tisangi 416206, MH, India
[c] Centre for Materials for Electronics and Technology (C-MET), Panchavati, Pune 411008, India

ARTICLE INFO

Article history:
Received 8 January 2016
Received in revised form
19 April 2016
Accepted 30 April 2016
Available online 3 May 2016

Keywords:
Nanoparticle synthesis
Cubic spinel
SEM
TEM
EDAX
Magnetic properties

ABSTRACT

Nanocrystalline $NiFe_{2-x}Mn_xO_4$ $(2 \geq x \geq 0)$ ferrites were prepared by sol–gel method. X-ray diffraction patterns reveal that synthesized compounds are in single phase cubic spinel lattice for all the composition. The surface morphology of all the samples were studied by scanning electron microscopy. The particle size measured from transmission electron microscopy and X-ray diffraction patterns confirms the nanosized dimension of the as-prepared powder. The elemental analysis was carried out by energy dispersive X-ray analysis technique. Magnetic properties such as saturation magnetization, coercivity and remanence are studied as a function of increasing Mn concentration at room temperature. The saturation magnetization shows a decreasing trend with increase in Mn content. The substitution of manganese in the nickel ferrite affects the structural and magnetic properties of cubic spinels.

1. Introduction

Mixed- metal oxides of nano size generated considerable interest because of their unique relationship between size and physico-chemical properties [1]. The synthesis, structural and magnetic characterization of spinel nano-ferrites have been studied by various investigators [2,3]. In magnetic nanoparticles, ferrimagnetisms and superparamagnetism are interesting phenomena [4–6]. In order to study the technological applications of magnetic nanomaterials such as data storage, [7] magnetocaloric refrigeration [8], drug delivery, medical diagnostics [9] and magnetic resonance imaging contrast enhancement [10] controlling and understanding of these behaviors are very important. Spinel compounds are ideal systems for investigating the relationship between magnetic properties and crystal chemistry of materials [11]. These properties are dependent on the nature of ions and their charge distribution among tetrahedral and octahedral sites. In spinels, the oxygen ions form a close packed cubic array, in which the A site cations occupy one-eighth of the tetrahedral sites while the B site cations are distributed over one half of the octahedral positions. And hence the change in the structural and magnetic properties of ferrites is due to substitution of different ions [12–15].

For the investigation of change in magnetization in a single-domain magnetic structure of the mixed spinel ferrite, the system $NiFe_{2-x}Mn_xO_4$.has been synthesized. Here, Fe^{3+} is partially replaced by Mn^{3+} which has a weaker magnetic moment than Fe^{3+}; that causes magnetic frustration. $NiFe_{2-x}Mn_xO_4$ nanoparticles should have a single domain magnetic structure, which might offer a simple system for understanding the magnetic behavior of all compositions. Also the oxides like nickel ferrite, nickel manganite display a negative temperature coefficient behavior where resistance decreases with increasing temperature. This makes the compound well suited for temperature sensing application [16].

2. Experimental details

During synthesis, powdered samples of the system $NiFe_{2-x}Mn_xO_4$, $(0.0 \leq x \leq 2.0)$ were synthesized by sol–gel method. High purity AR grade ferric nitrate, manganese nitrate, nickel nitrate and citric acid were used in the method of synthesis. The metal nitrate solutions were mixed in the required stoichiometric ratios in distilled water. The pH of the solution was maintained between 9 and 9.5 using ammonia solution. The solution was slowly heated around 373 K with constant stirring to obtain a floppy mass. The as synthesized precursor powder where $x=1.0$ was subjected to thermal analysis. The precursor powder was sintered at 973 K for

* Corresponding author.
E-mail addresses: p_hankare@rediffmail.com, pandavraj@rediffmail.com (P.P. Hankare).

http://dx.doi.org/10.1016/j.jmmm.2016.04.090
0304-8853/

8 h then mixed with 2% polyvinyl alcohol as a binder and uniaxially pressed at a pressure of 8 t/cm^2 to form the pellets.

The phase formation of the samples was confirmed by X-ray diffraction studies using Philips PW-1710 X-ray diffractometer with CuKα radiation ($\lambda = 1.54056$ Å).The surface morphology and elemental analysis of sintered powders were studied by using scanning electron microscopy (SEM Model - JEOL-JSM 6360) and energy dispersive X-ray analysis technique (EDAX). The nanosize of the particles was further confirmed by Philips 200 CX transmission electron microscope (TEM) by suspending the samples in isopropyl alcohol. Magnetic properties were studied using B–H loop tracer at a maximum applied field of 10 kOe.

3. Results and discussion

3.1. Thermal analysis

Thermogravimetric (TG) curve of an as synthesized $NiFe_{2-x}Mn_xO_4$ ferrite powder ($x = 1.0$) was recorded from the temperature range 10–1000 °C in air. Fig. 1 shows the thermogram with three major weight losses. A first weight loss observed below 227 °C is due to the evaporation of physically adsorbed water on the surface of the particles. Second and third weight losses are observed in the temperature range 227–384 °C. This weight loss corresponds to the decomposition of carbonaceous and nitrogenous material present in synthesized powder with liberation of CO_2, NOx etc. After 384 °C samples do not show any further weight loss and attain stability.

3.2. X-ray diffraction

X-ray diffraction patterns of Mn-substituted nickel ferrites are shown in Fig. 2. The values of lattice constant (a), crystallite size (t) X-ray density (dx) and bulk density (d_B) are calculated by using following equations and summarized in Table 1. From Table, it is showed that, all the samples of system are cubic and the lattice constant increases with substitution of manganese content. The increase in lattice constant with increase in Mn content is due to the higher ionic radii of Mn^{3+} (0.645 Å) ions as compared to Fe^{3+} (0.64 Å) ions (Table 1). Mn^{3+} ions have strong site preference energy for octahedral site; it tends to occupy the B site rather than A-site [17]. From the X-ray diffraction peaks, average particle size was estimated using Debye–Scherrer's formula.

$$t = 0.9\lambda/\beta \cos \theta \quad (1)$$

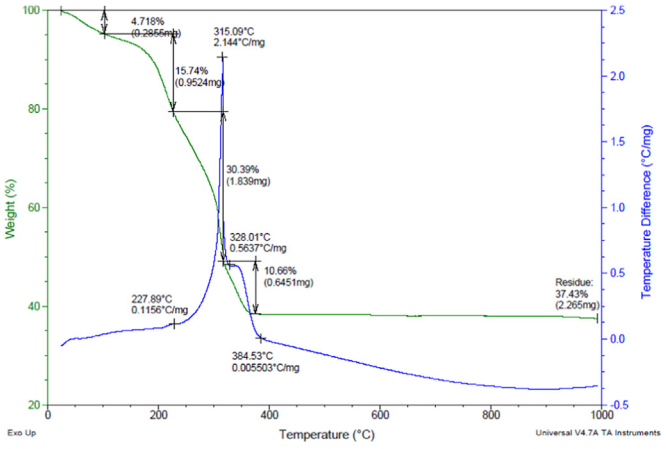

Fig. 1. TGA-DTA traces for the sample with $x = 1.0$.

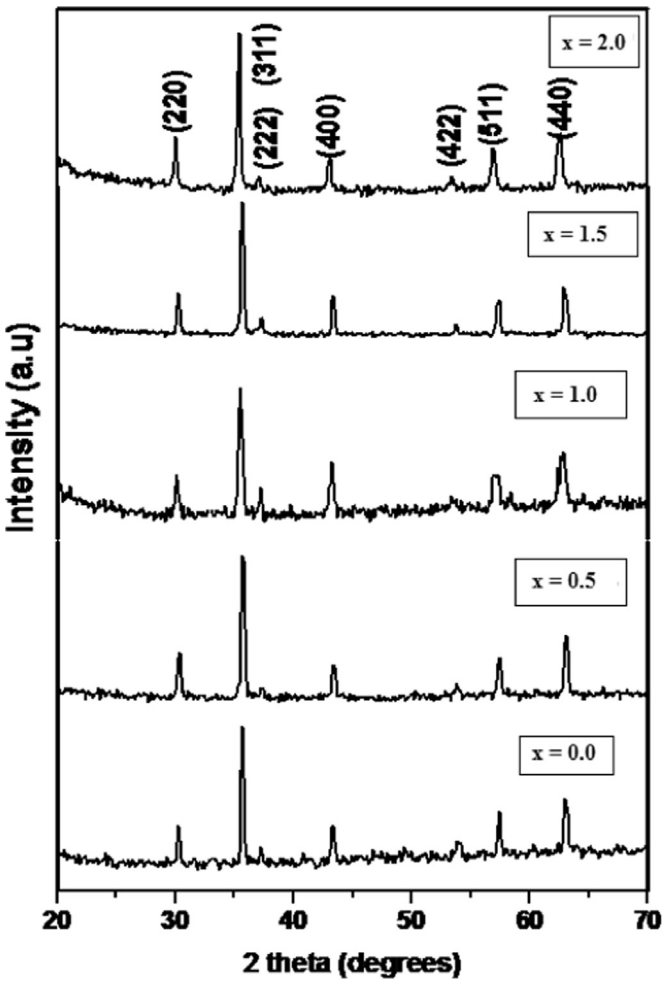

Fig. 2. X-ray diffraction patterns of $NiFe_{2-x}Mn_xO_4$ ferrite system.

where, symbols have their usual meaning.

The X-ray density (dx) was calculated using the following relation.

$$dx = 8M/Na^3 \quad (2)$$

where,

N = Avagadros number (6.023×10^{23} atom/mole)
M = Molecular weight in gm
a = Lattice constant.

The values of interplanar spacing (d), hkl planes and lattice constant (a) were obtained from XRD data with an accuracy of +0.03 Å. The linear increase in lattice constant with Mn content obeys Vegard's law and it is due to cationic size effect [18].

It is observed that X-ray density decreases with increase in Mn content, which may be due to the increase in lattice constant. The bulk density is lower than X-ray density which may be due to the presence of pores which are formed and developed during the sample preparation and sintering process. The substitution of Mn ions decreases the X-ray density and increases the porosity of the samples. This is because the sintering temperature of Mn_2O_3 is more than that of Fe_2O_3 [19].

The X-ray diffraction data was further used to confirm the single phase formation by calculating the tetrahedral and octahedral site radii (r_A and r_B). The site radii, r_A and r_B were calculated